Vibration Suppression of a Micropipe Conveying Fluid via Sliding Mode Technique

Zahra Jafari Shahbazzadeh[1*], Ramin Vatankhah[2], Mohamad Eghtesad[3]
1- School of Mechanical Engineering, Shiraz University, Shiraz, Iran.
Email: z_jafari.1993@yahoo.com (Corresponding author)
2- School of Mechanical Engineering, Shiraz University, Shiraz, Iran.
Email: rvatankhah@shirazu.ac.ir
3- School of Mechanical Engineering, Shiraz University, Shiraz, Iran.
Email: eghtesad@shirazu.ac.ir

Received: September 2018 Revised: January 2019 Accepted: March 2019

ABSTRACT:
In this article, derivation of a nonlinear model and nonlinear controller design for a micropipe conveying fluid, which is excited with a piezoelectric actuator, are accomplished. The governing equations are derived by using Hamilton's principle. The difference between the equations in micro-scales and macro-scales is established by using the modified couple stress theory. Unlike the classical Timoshenko beam theory, this new theorem includes a material length scale parameter which could help capturing the size effect. In addition, for thin members, so long as the deformation in the order of thickness, they do not remain in the elastic zone. Therefore, the linear theorem produces error in predicting in-plane movement of the member. In this way, the nonlinear terms are considered in the equations by applying mid-plane stretching theory. After this derivation, a frequency analysis is performed on the model. In addition, the effective parameters on the peak value of the response are studied as well. Finally, a sliding mode controller for the input voltage of the system is designed. It has been observed that by using this type of nonlinear controller, the behavior of the system could be improved significantly.

KEYWORDS: MEMS, Micropipe, Piezoelectric, Couple Stress Theorem, Hamilton's Principle, Sliding Mode Controller.

1. INTRODUCTION

Microstructure construction began with manufacturing microelectronic components such as ICs and semiconductors [1]. This technology has been expanded to other fields such as micromechanics techniques. The effective searches about micromechanics was done in 1970s [2]. Micromechanics methods relate to the technology of using Silicon as a mechanical material because of small dimensions [3]. Fabrication of MEMS was one of the most helpful inventions for scientists. It has different application: in biotechnology, MEMS is absolutely useful for drug delivery [4]. Also, MEMS pressure sensors are widely used for decades in medical science [5]. MEMSs have largely used as inertial sensors such as accelerometers and gyroscopes [6].

The difference between the size (scale order) of structures, leads to different behaviors. It is observed that the smaller thickness of pipe causes the more different material behavior [7]. In the case of small thickness, classical modelling theories of structures cannot support these new systems which can capture size of the system. In order to formulize these systems, there exists many different continuum theories which can consider size effect. Modified couple stress theory and modified strain gradient elasticity are two examples. In modified couple stress theory, with the aid of "microstructure length scale parameter" which is added to the model because of considering von Karman geometric nonlinearity, a more precise deflection prediction occurs [8]. This parameter results in the increase in the bending rigidity of the model with respect to classical models [7]. This modification theory can be used for both classical Timoshenko beam theory [9] and Euler-Bernoulli beam theory [10]. In modified strain gradient theory, the same length scale parameter exists. However, the different definition of strain energy causes different governing equation, the sixth order equations [11].

As this system itself has unstable behavior, it needs an actuator that can control the response. Among different actuator material such as piezoelectric materials, shape memory alloys, electrostrictive materials, magnetostrictive materials, electro-

rheological fluids, and fiber optics [12], in this paper a piezoelectric actuator is used. [13] and [14] and [15] are some example researches of using piezoelectric materials as actuators for cylindrical systems.

Considering the relation of exciting force of the system, voltage can be used as the control signal. As the governing equations are nonlinear, using a nonlinear controller can have better results. Sliding mode controller is one of the most popular nonlinear controllers. However, because of difficulties of this type of controller, including; handle the uncertainty bounds and removing chattering phenomenon, it is usually combined with other controllers. Neuro- sliding mode controller [16], adaptive sliding mode controller [17] and fuzzy sliding mode controller [18] are some examples of this. Through these different nonlinear controllers, in the current research "fuzzy sliding mode control" or FSMC is utilized. Using a fuzzy tuning scheme can help to improve the performance of the control system [19].

2. MODELLING

As the studied model contains a micropipe and a piezoelectric actuator, mathematical modelling of this system has two separate parts.

2.1. Modelling of Micropipe Conveying Fluid

For a better understating, the physical and material properties of the system is written in the following table:

Table 1. The properties of the model.

E	Young's modulus	A	Cross sectional area
G	Shear modulus	L	Length of the pipe
m	Mass per unit length of fluid	I	Second moment of inertia of pipe
M	Mass per unit length of pipe	U	Fluid velocity
l	Material length scale	ρ_f	Density of fluid

And the schematic of the hollow pipe having simply supported ends is shown in Fig. 1.

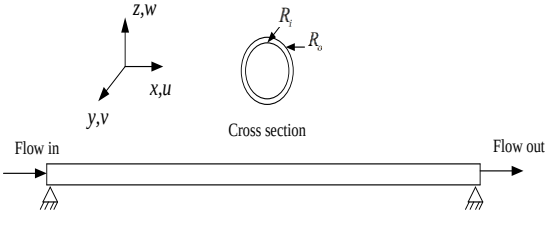

Fig. 1. The schematic of the system.

In order to develop the mathematical model of the system the following assumptions are considered:

1- The conveying fluid is incompressible.
2- The radius to length ratio is high.
3- Shear deformation and rotary inertia are negligible.

The last assumption leads for using the Euler-Bernoulli beams theory.

As it is discussed in the introduction, for illustrating the difference between micro- and macro-scale properties of beams, the non-classical continuum theories should be used. Modified couple stress theory and strain gradient theory are two examples of these theories which the first one is utilized in this paper. This theory adds a 'material length scale' parameter to the classic model which could capture the size effect. It should be noted that the difference between two models becomes more significant when the thickness of the pipe is small and this behavior returns to the intrinsic property of the pipe [20]. In order to derive the equations using Hamilton's principle, strain potential energy of the system should be written. Base on this theorem the size-dependent strain energy is:

$$U = \frac{1}{2}\int_V \left(\sigma_{ij}\varepsilon_{ij} + m_{ij}\chi_{ij}\right)dv \quad i, j = 1,2,3 \tag{1}$$

In which V is the occupying volume, σ_{ij} is element of Cauchy stress tensor, ε_{ij} is element of the strain tensor, χ_{ij} is the element of symmetric curvature tensor and finally m_{ij} is the element of deviatoric part of the couple stress tensor. The strain field tensors, according to [21], are written in equations (2) and (3).

$$\varepsilon_{ij} = \frac{1}{2}\left[\nabla u_i + \left(\nabla u_j\right)^T\right] \tag{2}$$

$$\chi_{ij} = \frac{1}{2}\left[\nabla \theta_i + \left(\nabla \theta_j\right)^T\right] \tag{3}$$

$$\theta_i = \frac{1}{2} curl\left(u_i\right) \tag{4}$$

In the above equations, u_i and θ_i are displacement vector and rotation vector, respectively.

The relationship between stress and strain from constitutive equations is as follows.

$$\sigma_{ij} = \lambda tr\left(\varepsilon_{ij}\right)\delta_{ij} + 2G\varepsilon_{ij} \quad , \quad m_{ij} = 2l^2 G\chi_{ij} \tag{5}$$

λ and G represent the Lame's constants (shear modulus is one of the Lame's constants),l is material length scale parameter and δ_{ij} is the Kronecker's delta function.

Using the above relations, among the stress and strain elements, the non-zero terms of these fields are as follows.

$$\sigma_{xx} = E\left[\frac{\partial u_0}{\partial x} + \frac{1}{2}\left(\frac{\partial w_0}{\partial x}\right)^2 - z\frac{\partial^2 w_0}{\partial x^2}\right], \quad (6)$$

$$m_{xy} = m_{yx} = -Gl^2\frac{\partial^2 w_0}{\partial x^2}$$

$$\varepsilon_{xx} = \frac{\partial u_0}{\partial x} + \frac{1}{2}\left(\frac{\partial w_0}{\partial x}\right)^2 - z\frac{\partial^2 w_0}{\partial x^2}, \quad (7)$$

$$\chi_{xy} = \chi_{yx} = -\frac{1}{2}\frac{\partial^2 w_0}{\partial x^2}$$

Substituting all stress-strain relations into equation (1), the strain potential energy is:

$$U = \frac{1}{2}\int_0^L \left\{EA\left[\frac{\partial u_1}{\partial x} + \frac{1}{2}\left(\frac{\partial u_3}{\partial x}\right)^2\right]^2 + \left(EI + GAl^2\right)\left(\frac{\partial^2 u_3}{\partial x^2}\right)^2\right\}dx \quad (8)$$

In addition to strain energy, the total kinetic energy of the system, the virtual work done by external force and the wasted energy of the damper should be calculated.

$$T_p = \frac{1}{2}m\int_0^L\left[\left(\frac{\partial u_3}{\partial t}\right)^2 + \left(\frac{\partial u_1}{\partial t}\right)^2\right]dx$$

$$T_f = \frac{1}{2}M\int_0^L\left\{\left[\frac{\partial u_1}{\partial t} + U\left(1 + \frac{\partial u_1}{\partial x}\right)\right]^2 + \left[\frac{\partial u_3}{\partial x} + U\frac{\partial u_3}{\partial x}\right]^2\right\}dx \quad (9)$$

$$\delta W_f = \int_0^L f\left(x,t\right)\delta\bar{u}dx, \quad (10)$$

$$\delta W_D = \int_0^L c_w\frac{\partial u_3}{\partial t}\delta u_3 dx$$

p and *f* indices stand for pipe and fluid, respectively. In relation (10), $\bar{u}$ is the displacement of the actuator which will be discussed in the next part.

2.2. Modelling of the Piezoelectric Actuator

The external force in this model is exerted using a piezoelectric which is oriented in longitudinal direction as shown in Fig. 2.

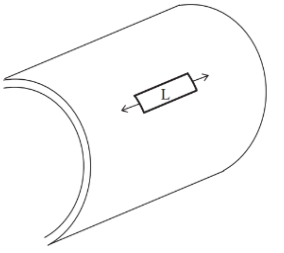

Fig. 2. Longitudinal piezoelectric.

The surface displacement of the pipe relates to this type of piezoelectric actuator and also the magnitude of this time dependent force is:

$$\bar{u} = u - \frac{h}{2}\frac{\partial w}{\partial x},\ f\left(t\right) = E_p d_{33} V_{pa} \quad (11)$$

In which, E_p is the Young's modulus of the piezoelectric material, d_{33} is the piezoelectric constant and V_{pa} is the applied voltage which is control signal in this issue.

Inserting all these parts in Hamilton's equation as following:

$$\delta\int_{t_1}^{t_2}\left(T_p + T_f - U\right)dt + \int_{t_1}^{t_2}\left(\delta W_f + \delta W_D\right)dt = 0 \quad (12)$$

Simplifying the above equation, two equations of motion are as follows. (the zero subscript is omitted.)

$$-\frac{\partial}{\partial x}\left\{EA\left[\frac{\partial u}{\partial x} + \frac{1}{2}\left(\frac{\partial w}{\partial x}\right)^2\right]\right\} + \alpha M\bar{U}^2\frac{\partial^2 u}{\partial x^2} + 2M\bar{U}\frac{\partial^2 u}{\partial t\partial x} + \left(m + M\right)\frac{\partial^2 u}{\partial x^2} = f\left(x,t\right) \quad (13)$$

$$\left(EI + GAl^2\right)\frac{\partial^4 w}{\partial x^4} + \alpha M\bar{U}^2\frac{\partial^2 w}{\partial x^2} + \left(m + M\right)\frac{\partial^2 w}{\partial t^2} = f_2\left(x,t\right) = \frac{h}{2}\frac{\partial}{\partial x}f\left(x,t\right) \quad (14)$$

Using the boundary condition equations (which are not written here) and also neglecting the axial displacement in order to have more simple equations, the final partial differential equation and its BC equations are:

$$\left(EI + GAl^2\right)\frac{\partial^4 w}{\partial x^4} + \left[\alpha M\bar{U}^2 - \frac{EA}{2L}\int_0^L\left(\frac{\partial w}{\partial x}\right)^2 dx\right]\frac{\partial^2 w}{\partial x^2} + c_w\frac{\partial w}{\partial t} + 2M\bar{U}\frac{\partial^2 w}{\partial t\partial x} + \left(m + M\right)\frac{\partial^2 w}{\partial t^2} = f_2\left(x,t\right) \quad (15)$$

$$-\left(EI+GAl^2\right)\frac{\partial^3 w}{\partial x^3}-\alpha M\bar{U}^2\frac{\partial w}{\partial x}-M\bar{U}\frac{\partial w}{\partial t}+ \quad (16)$$
$$\frac{EA}{2L}\left[\int_0^L\left(\frac{\partial w}{\partial x}\right)^2 dx\right]\frac{\partial w}{\partial x}=0 \text{ or } w=w_s$$

$$\left(EI+GAl^2\right)\frac{\partial^2 w}{\partial x^2}=0 \text{ or } \frac{\partial w}{\partial x}=\frac{\partial w_s}{\partial x} \quad (17)$$

2.3. Discretizing the Equation of Motion

In order to solve the governing equation (15) having infinite degrees of freedom absolutely needs a numerical solving method. Using Galerkin method, the PD equation can be converted to a number of ODEs. As this equation has lots of parameters before applying Galerkin's method, the nondimensionalized equations are extracted.

In the Galerkin's method the lateral displacement is approximated with this series:

$$\eta(\zeta,t)=\sum_{i=1}^{N}\varphi_i(\zeta)\,p_i(\tau) \quad (18)$$

In which η is the nondimension-lateral displacement, p_n means the n^{th} generalized coordinate of lateral motion and φ_n is the n^{th} linear undamped eigenfunction for the lateral motion of the system. For this problem one of the adequate eigenfunctions, which satisfies the boundary conditions, is:

$$\varphi_i(\zeta)=\sin(\pi i\zeta) \quad (19)$$

Substituting all of these relations in the nondimension equation, the discretized ordinary equation is in the form of:

$$\mathbf{M}_{ij}\ddot{p}_j+\mathbf{C}_{ij}\dot{p}_j+\mathbf{K}_{ij}p_j+\mathbf{K}_{3_{ijkl}}p_j p_k p_l=\mathbf{F}_i \quad (20)$$
$$i=1,2,...,N$$

Where the components of matrices can be calculated as:

$$\mathbf{M}_{ij}=\int_0^1\varphi_i\varphi_j d\zeta$$
$$\mathbf{C}_{ij}=2\bar{V}\sqrt{\beta}\int_0^1\varphi_i\frac{\partial\varphi_j}{\partial\zeta}d\zeta+c_d\int_0^1\varphi_i\varphi_j d\zeta$$
$$\mathbf{K}_{ij}=(1+\theta)\int_0^1\varphi_i\frac{\partial^4\varphi_j}{\partial\zeta^4}d\zeta+\bar{V}^2\int_0^1\varphi_i\frac{\partial^2\varphi_j}{\partial\zeta^2}d\zeta \quad (21)$$
$$\mathbf{K}_{3_{ijkl}}=-\frac{S^2}{2}\left(\int_0^1\varphi_i\frac{\partial^2\varphi_l}{\partial\zeta^2}d\zeta\right)\left(\int_0^1\frac{\partial\varphi_j}{\partial\zeta}\frac{\partial\varphi_k}{\delta\zeta}d\zeta\right)$$
$$\mathbf{F}_i=\int_0^1\bar{f}\varphi_i d\zeta$$

2.4. Control

In this paper, sliding mode controller is applied to the required voltage of the system. Having a brief review on this type of controller; a general form for a SISO system is:

$$x^{(n)}=f(\underset{\sim}{x})+b(\underset{\sim}{x})u \quad (22)$$

In this controller, the aim is to reduce the distance between the state vector (x) and its desired vector (x_d). In this way a sliding surface (s) is defined for a nth order system and the goal alters to reaching to this surface:

$$s\equiv 0 \qquad \text{where} \qquad \mathrm{s}(x,t)=\left(\frac{d}{dt}+\lambda\right)^{n-1}\underset{\sim}{x} \quad (23)$$

Using Lyapunov theorem, if a positive Lyapunov function V is defined; a negative derivation of V makes s go to zero. For instance, if this function be defined as the squared distance from the surface:

$$V=\frac{1}{2}s^2,\dot{V}=\frac{1}{2}\frac{d}{dt}s^2\le 0 \quad (24)$$

The second condition is replaced by a more conservative condition as follows:

$$\dot{V}=\frac{1}{2}\frac{d}{dt}s^2\le-\eta|s| \quad (25)$$

For a second order system as above, the following discontinuous control signal satisfies the sliding condition:

$$u=b^{-1}\left(\ddot{x}_d-f(x)-\lambda\dot{\underset{\sim}{x}}-ksat\left(\frac{s}{\varphi}\right)\right) \quad (26)$$

.

3. RESULTS

3.1. Verifying the Model

In the current paper, just one mode is considered for the model. First of all, the model was verified using the results of [22]. As an example, in Fig. 3, variation of the first natural frequency in term of increasing the velocity is shown which is exactly coincides with the figure number 2 in [22]. (For avoiding redundancy, other figures are not brought here.)

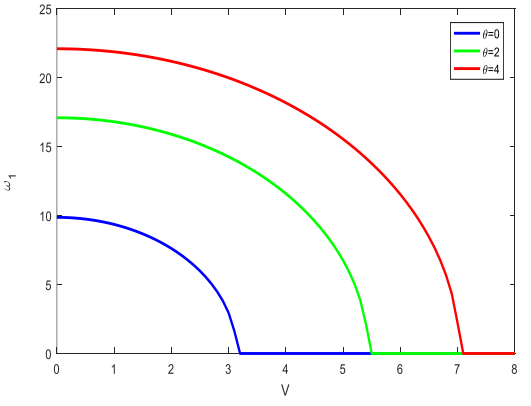

Fig. 3. First frequency as the function of velocity.

3.2. Results of the Controlling Method

After checking the model, the controller should be applied. The value of the parameters are used in the matrices, as following:

Table 2. Numerical value of parameters of the model.

E	1.44×10^{9} pa	I	3.96×10^{-17} m^4
A	3.2835×10^{-8}m	m	8.9×10^{-6} kg/m
G	5.22×10^{8}pa	M	4.01×10^{-5} kg/m
L	8.8 mm	U	1 m/s
l	1.76×10^{-5}	c_w	0.04

The lateral displacement of the micropipe is plotted versus time for the case of uncontrolled pipe (Fig. 4) and also the controlled pipe (Fig. 5) in the following. The explained fuzzy-sliding mode control is applied to the model.

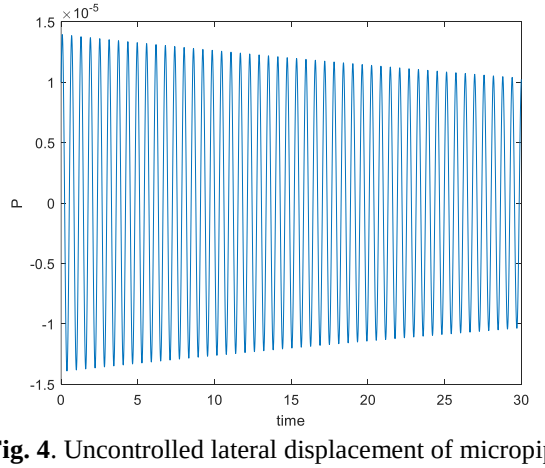

Fig. 4. Uncontrolled lateral displacement of micropipe.

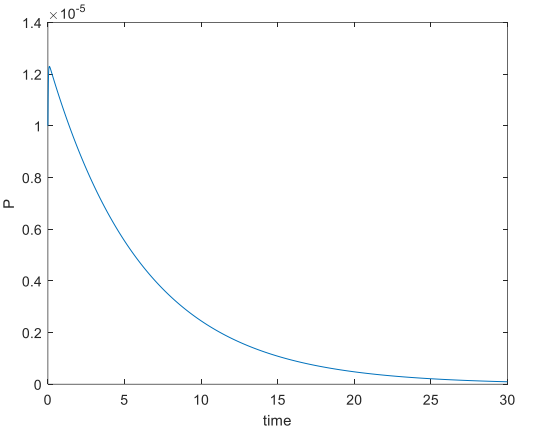

Fig. 5. Controlled lateral displacement of micropipe.

4. CONCLUSION

Form the drawn figures, it can be seen that using sliding mode controller, can lead to have a "better performance". For such a system, the meaning of better performance is removing all oscillations and also having a lower settling time in comparison with the uncontrolled results. Although this controller has absolutely acceptable results, the fuzzy system can be added in order to improve the above-mentioned performance properties and maybe some other properties. In this way, manipulating the parameter of sliding mode controller can be useful.

REFERENCES

[1] K. Subramani and W. Ahmed, **"Emerging Nanotechnologies in Dentistry: Processes, Materials and Applications"**, *William Andrew*, 2011.

[2] K. E. Petersen, **"Petersen, Kurt E. "Dynamic Micromechanics on Silicon: Techniques and Devices,"** *IEEE Trans. Electron Devices*, Vol. 25, No. 10, pp. 1241–1250, 1978.

[3] L. Csepregi, **"Micromechanics: A Silicon Microfabrication Technology,"** *Microelectron. Eng.*, Vol. 3, No. 1–4, pp. 221–234, 1985.

[4] N. M. Elman and U. M. Upadhyay, **"Medical Applications of Implantable Drug Delivery Microdevices Based on MEMS (Micro-Electro-Mechanical-Systems),"** *Curr. Pharm. Biotechnol.*, Vol. 11, No. 4, pp. 398–406, 2010.

[5] W. P. Eaton and J. H. Smith, **"Micromachined Pressure Sensors: Review and Recent Developments,"** *Smart Mater. Struct.*, Vol. 6, No. 5, p. 530, 1997.

[6] O. Brand, I. Dufour, H. Stephen, and J. Fabien, Resonant **"MEMS: Fundamentals, Implementation, and Application",** *John Wiley & Sons*, 2015.

[7] S. K. Park and X. L. Gao, **"Bernoulli-Euler Beam Model Based On A Modified Couple Stress Theory,"** *J. Micromechanics Microengineering*, Vol. 16, No. 11, pp. 2355–2359, 2006.

[8] A. Arbind , J. N. Reddy, **"Nonlinear Analysis Of Functionally Graded Microstructure-Dependent Beams,"** *Compos. Struct.*, Vol. 98, pp. 272–281, 2013.

[9] H. M. Ma, X. L. Gao, and J. N. Reddy, **"A Microstructure-Dependent Timoshenko Beam Model Based On A Modified Couple Stress Theory,"** *J. Mech. Phys. Solids*, Vol. 56, No. 12, pp. 3379–3391, 2008.

[10] B. Akgöz and Ö. Civalek, **"Free Vibration Analysis of Axially Functionally Graded Tapered Bernoulli-Euler Microbeams Based on the Modified Couple Stress Theory,"** *Compos. Struct.*, Vol. 98, pp. 314–322, 2013.

[11] R. Vatankhah, A. Najafi, H. Salarieh, and A. Alasty, **"Boundary Stabilization of Non-Classical Micro-Scale Beams,"** *Appl. Math. Model*., Vol. 37, No. 20–21, pp. 8709–8724, 2013.

[12] M. K. Kwak, S. Heo, and M. Jeong, **"Dynamic Modelling And Active Vibration Controller Design for A Cylindrical Shell Equipped with Piezoelectric Sensors And Actuators,"** *J. Sound Vib*., Vol. 321, No. 3–5, pp. 510–524, 2009.

[13] V. R. Sonti and J. D. Jones, **"Active Vibration Control of Thin Cylindrical Shells Using Piezo-Electric Actuators,"** *Proc. Conf. Recent Adv. Act. Control Sound Vib. Virginia Polytech. Inst. State Univ*. Blacksburg, VA, pp. 21–38, 1991.

[14] H. C. Lester and S. Lefebvre, **"Piezoelectric Actuator Models for Active Sound and Vibration Control of Cylinders,"** *J. Intell. Mater. Syst. Struct*., Vol. 4, No. 3, pp. 295–306, 1993.

[15] R. L. Clark and C. R. Fuller, **"Active Control of Structurally Radiated Sound from an Enclosed Finite Cylinder,"** J. Intell. Mater. Syst. Struct., Vol. 5, No. 3, pp. 379–391, 1994.

[16] Y. Yildiz, A. Sabanovic, and K. Abidi, **"Sliding-Mode Neuro-Controller for Uncertain Systems,"** *IEEE Trans. Ind. Electron.*, Vol. 54, No. 3, pp. 1676–1685, 2007.

[17] H. Xu, M. D. Mirmirani, and P. A. Ioannou**, "Adaptive Sliding Mode Control Design for a Hypersonic Flight Vehicle,"** *J. Guid. Control. Dyn*., Vol. 27, No. 5, p. 829–838., 2004.

[18] A. Shahraz and R. Bozorgmehry Boozarjomehry, **"A Fuzzy Sliding Mode Control Approach For Nonlinear Chemical Processes,"** *Control Eng. Pract*., Vol. 17, No. 5, pp. 541–550, 2009.

[19] H. Q. T. N. Shin, Jin-Ho, and W.-H. Kim, **"Fuzzy Sliding Mode Control For A Robot Manipulator,"** *Artificial Life Robot*., Vol. 13, No. 1, pp. 124–128, 2008.

[20] S. K. Park and X. Gao, **"Bernoulli – Euler Beam Model Based On A,"** Vol. 2355, pp. 0–5, 2006.

[21] Lai, W. M., Rubin, D. H., Krempl, E., & Rubin, D., **"Introduction to Continuum Mechanics",** *Butterworth-Heinemann*, 2009.

[22] A. M. Dehrouyeh-Semnani, M. Nikkhah-Bahrami, and M. R. H. Yazdi, **"On Nonlinear Vibrations of Micropipes Conveying Fluid,"** *Int. J. Eng. Sci.*, Vol. 117, pp. 20–33, 2017.